European Heart Journal Advance Access published March 18, 2009

European Heart Journal
doi:10.1093/eurheartj/ehp062

CLINICAL RESEARCH

# Apical transverse motion as surrogate parameter to determine regional left ventricular function inhomogeneities: a new, integrative approach to left ventricular asynchrony assessment

**Jens-Uwe Voigt[1]*†, Thomas-Michael Schneider[2]†, Stephan Korder[2], Mariola Szulik[1], Emre Gürel[1], Werner G. Daniel[2], Frank Rademakers[1], and Frank A. Flachskampf[2]**

[1]Department of Cardiology, University Hospital Gasthuisberg, Cath. University Leuven, Herestraat 49, 3000 Leuven, Belgium; and [2]Medical Clinic II, University Hopital Erlangen, Friedrich-Alexander-University Erlangen-Nürnberg, Ulmenweg 18, 91054 Erlangen, Germany

*Received 26 June 2008; revised 22 January 2009; accepted 30 January 2009*

**This paper was guest edited by Dr Michael H. Picard, Department of Cardiology, Massachusetts General Hospital, Boston, USA**

**Aims** Left ventricular (LV) asynchrony assessment is mostly based on delays between regional myocardial velocity peaks. Regional function is barely considered. We propose apical transverse motion (ATM) as a new parameter integrating both temporal and functional information, which was tested in different conduction delays.

**Methods and results** We examined 67 patients, 11 patients with post-infarct ischaemic left bundle branch blocks (iLBBB) and 25 patients with non-ischaemic left bundle branch block (nLBBB), 12 patients with right bundle branch block (RBBB), and 19 normal healthy volunteers (NORM). Longitudinal colour tissue Doppler data were used to calculate the total transverse apex motion (ATM), the transverse motion in the four-chamber view plane alone ($ATM_{4CV}$) as well as regional myocardial deformation and conventional LV asynchrony parameters. Median ATM was 1.8 mm in NORM, 1.5 mm in RBBB ($P = 0.999$), 2.4 mm in iLBBB ($P = 0.183$), and 4.3 mm in nLBBB ($P < 0.001$ vs. NORM and RSB). $ATM_{4CV}$ behaved similarly, showed a good correlation with regional deformation data, and distinguished well between NORM and LBBB (AUC = 0.87).

**Conclusion** Apical transverse motion is a new and simple parameter integrating information on both regional and temporal function inhomogeneities of the LV. It has a potential role in assessing LV asynchrony in the clinical context.

**Keywords** Myocardial function • Dyssynchrony • Conduction delay

## Introduction

Regional mechanical left ventricular (LV) dysynchrony plays an important role in the aetiology of LV dysfunction and heart failure. Both regional myocardial dysfunction, as it occurs e.g. in infarcted myocardium, and myocardial activation inhomogeneities, as e.g. in left bundle branch blocks (LBBB), will result in an inhomogeneous contraction of the LV myocardium with unfavourable re-distribution of loading and subsequent inhomogeneous regional remodelling.[1] This remodelling leads to further functional deterioration of early or less contracting regions and causes inefficient LV performance.

With the introduction of cardiac resynchronization therapy (CRT) as a therapeutic option to re-synchronize the contraction of LV regions, the correct characterization of regional function inhomogeneities has become a new task of non-invasive imaging. Owing to its wide availability and potential to image and quantify regional function with good spatial and excellent temporal

* Corresponding author. Tel: +32 16 349 016, Fax: +32 16 344 240, Email: jens.uwe.voigt@gmx.net

† The first two authors contributed equally to the study.

**Table 1 Characteristics of the study population**

| | *n* | age (years) | EF (%) | Sign[a] (*P*-value) | QRS width (ms) | Sign[a] (*P*-value) |
|---|---|---|---|---|---|---|
| NORM | 19 | 35 ± 12 | 62 ± 6 | | 98 ± 9 | |
| RBBB | 12 | 63 ± 13 | 63 ± 6 | 0.989 | 150 ± 13 | < 0.001 |
| nLBBB | 25 | 63 ± 13 | 23 ± 11 | < 0.001 | 167 ± 19 | < 0.001 |
| iLBBB | 11 | 69 ± 8 | 23 ± 17 | < 0.001 | 155 ± 19 | < 0.001 |

[a]vs. NORM. Ejection fraction (EF) was not significantly different between the two LBBB groups. QRS width was not significantly different between the three patients groups.

resolution, echocardiography is usually the method of choice. Two questions have to be answered in asynchrony analysis: (i) is there a temporal inhomogeneity in regional myocardial contraction? and (ii) is there a regional inhomogeneity in residual myocardial function? The first question is usually easy to answer, whereas answering the second is difficult because of the marked interaction of myocardial regions during the cardiac cycle.

In the past, several proposals have been made to approach LV asynchrony. Most suggestions were based on the analysis of the occurrence of myocardial velocity peaks measured by Tissue Doppler. This approach allows to assess timing inhomogeneities within the LV.[2–6] Owing to interaction between regions (tethering), a reliable analysis of the true regional function is difficult. Accordingly, more recent reports have dampened the enthusiasm about the clinical value of these parameters.[7] Other authors analysed regional motion with 3D echo[8] or looked at deformation.[9] These approaches allow an estimation of the contraction sequence within the LV, but hardware demands, limited temporal resolution or noisy data remain the problems of such approaches.

Herewith, we propose a new, integrative, and thus, simple parameter for assessing regional myocardial function inhomogeneities. Apical transverse motion (ATM), a motion of the LV apical myocardium perpendicular to the LV long axis (apical 'rocking'), is an often observed phenomenon in asynchronously contracting ventricles. Apical transverse motion, if caused by asynchronous contraction of the different LV regions, would integrate both information on residual contractile function of the myocardium and on the temporal sequence of regional mechanical activation. With this study, we investigated ATM in normal hearts and different pathological entities.

# Methods

## Study population

The study population comprised 67 subjects, which is comparable to previously published studies in the field of echocardiographic asynchrony assessment.

A group of 19 normal healthy volunteers (NORM) without any history of cardiovascular disease, without abnormal findings during physical examination, with normal ECG at rest and during bicycle stress, and normal results of a standard echocardiogram was studied.

Furthermore, 25 patients with non-ischaemic LBBB (nLBBB) were included. A coronary angiogram ruled out coronary artery disease in all of them. Eleven patients with chronic ischaemic LBBB (iLBBB) were also studied. All had documented myocardial infarction at least 1 year prior to the study examination. A current relevant coronary artery stenosis was ruled out by non-invasive stress testing or coronary angiography. Finally, we included 12 patients with right bundle branch block (RBBB). In those, ischaemia inducing coronary artery disease was excluded by non-invasive testing or coronary angiography.

No patient had more than mild valve disease or more than mild pulmonary hypertension. All patients were in sinus rhythm. None had ventricular arrhythmias exceeding occasional premature beats. Patients were included irrespective of their LV ejection fraction (EF). No patient was paced. Characteristics of the groups are summarized in *Table 1*. All study participants gave informed consent prior to inclusion.

## Selection of study subjects

Volunteers were recruited from a group of hobby speologists comprising healthy adults in good physical shape in a wide age range. Patients were recruited via the ECG service of the Medical Clinic II in Erlangen. Patients with an QRS width of >130 ms were transferred to the echo lab for a screening echo to evaluate image quality and to exclude major valve disease. We initially aimed at 60 participants. When this number was reached, we focused on selective inclusion of additional iLBBB and RBBB patients who were underrepresented. Inclusion was stopped, when all groups comprised >10 subjects.

## Echocardiography

All patients were scanned after 5 min of rest in a left lateral decubitus position. We used a Vivid 7 ultrasound scanner (GE Vingmed, Horton, Norway) to perform a standard echocardiogram and to acquire grey scale and colour Doppler myocardial imaging (DMI) data from an apical two-, three-, and four-chamber view. For DMI data acquisition, care was taken to maximize frame rate by reducing depth and sector angle (typical frame rate: 100 fps). Blood pool Doppler traces of all valves were used to determine valve openings and closures. All acquired image loops contained at least three cardiac cycles. Data were digitally stored for later off-line analysis.

## Post-processing and measurements

As a first step, we used an EchoPac workstation (GE Vingmed) to review the data and to measure cardiac diameters from a parasternal long-axis view. Ejection fraction was determined according to the bi-plane Simpson's method from apical images. Regional wall motion was scored as normo-, hypo-, a-, and dyskinetic using a modified 18 segment model.

Secondly, we extracted myocardial velocity and strain rate traces from the lower half of the apical, medial, and basal segments as well as the mitral ring of each myocardial wall (septal, anteroseptal, anterior, lateral, posterior, inferior). Thus, the same 18-segment model was used for Doppler data analysis. The position of the regions of interest (ROI) was manually adjusted during the cardiac

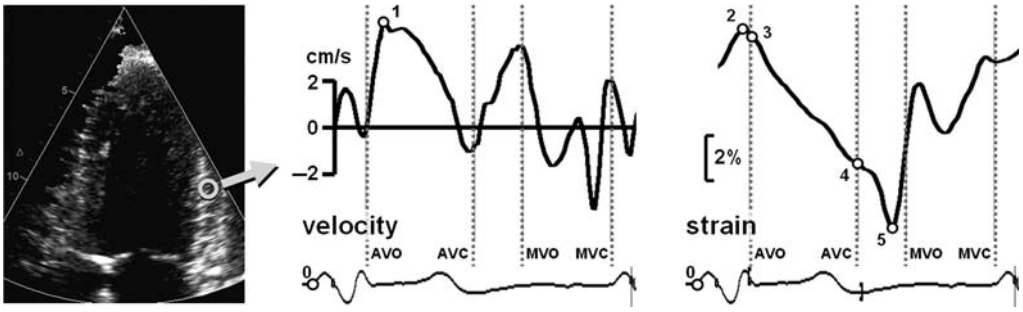


**Figure 1** Longitudinal velocity and strain curve examples from a lateral wall region of interest with typical position of measurement points: (0) onset of QRS, (1) peak systolic velocity, (2) onset of shortening, curve maximum, (3 and 4) strain at the begining and end of ejection, (5) maximal shortening, curve minimum. AVO, AVC, MVO, MVC—opening and closure of aortic and mitral valve as derived from spectral Doppler. Time-to-peak systole is calculated as $t_{sys} = t_1 - t_0$; time to onset of shortening as $t_{onset} = t_2 - t_0$; time to end of shortening as $t_{end} = t_5 - t_0$. Deformation is calculated as $\epsilon_{tot} = \epsilon_5 - \epsilon_2$ and $\epsilon_{et} = \epsilon_4 - \epsilon_3$.

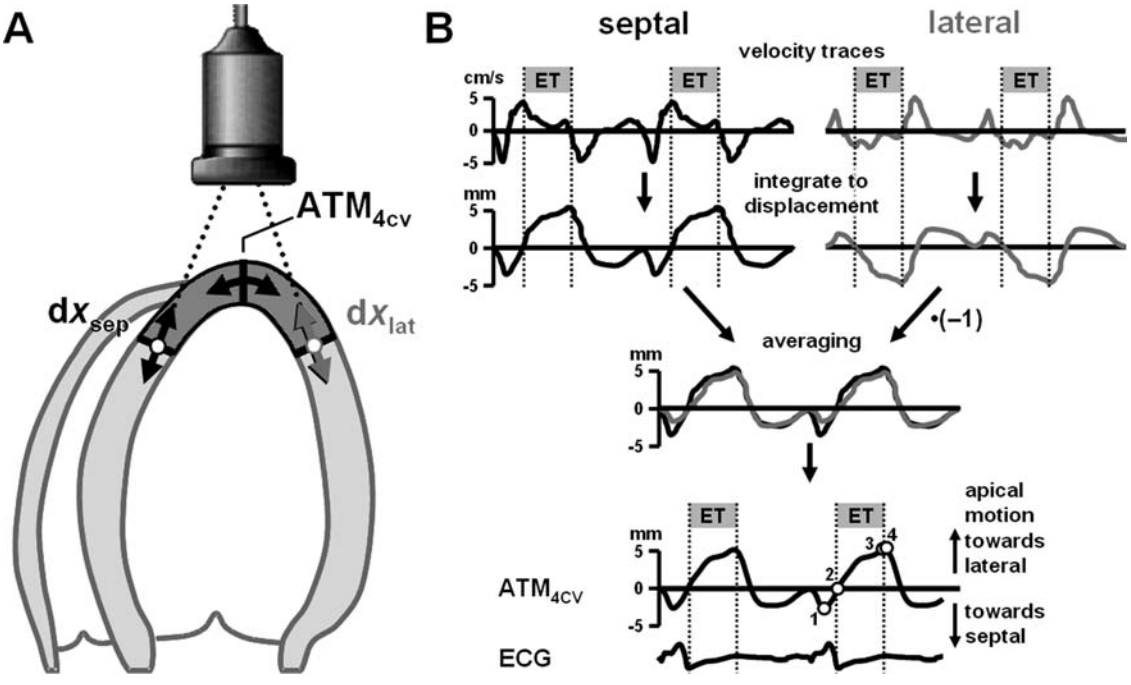


**Figure 2** Data acquisition and ATM calculation, exemplified for the two-chamber view. Data from apical long axis and two-chamber views are processed likewise. (*A*) Assuming that the transverse apex motion in the four-chamber view is the average of the longitudinal apical septal and the inverted apical lateral motion, longitudinal velocity traces are obtained in the two apical segments by tissue Doppler. (*B*) For ATM calculation, velocity traces are integrated to displacement traces. After inversion of the lateral, curves can be averaged to obtain the ATM in the plane of the four-chamber view. The numbers in the ATM curve indicate the measurement positions to measure the total amplitude of ATM (Point 4 – Point 1) and ATM during ejection time (ET) (Point 3 – Point 2). The example shows a typical LBBB pattern with early short septal motion of the apex during isovolumic contraction time and lateral motion during the entire ejection time.

cycle to follow myocardial motion and to ensure a constant mid-wall position of the ROI.

In a third step, traces were imported in a dedicated, Matlab (the Math Works Inc., Natick, MA, USA) based analysis software (TVA version 14.3, JU Voigt, University Leuven, Belgium), which allowed to calculate and baseline-correct motion and strain traces and to calculate ATM. From segmental velocity curves, we extracted amplitude and timing of the systolic ($v_{sys}$, $t_{sys}$) peak. From strain curves, we determined the timing of the onset ($t_{onset}$) and end of systolic shortening ($t_{end}$) as well as the amplitude of shortening during ejection time

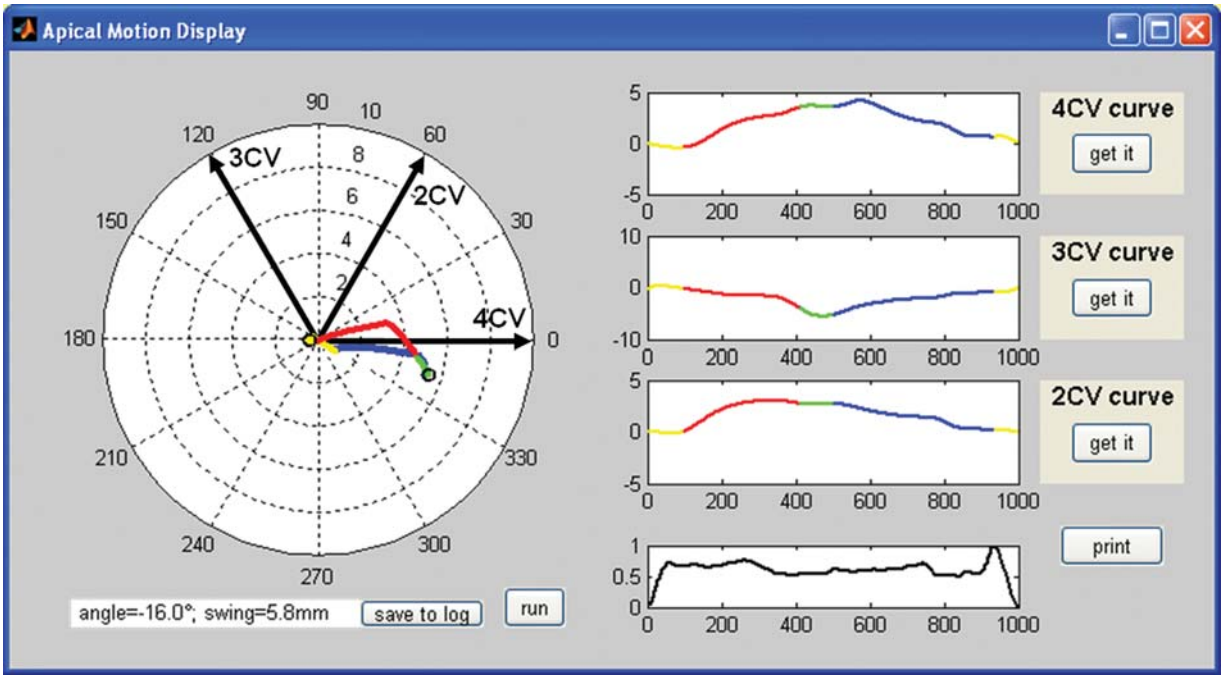


**Figure 3** Screenshot of ATM loop reconstruction tool with data from a patient with LBBB. The polar plot on the left shows the transverse (perpendicular to the LV long axis) displacement of the apex (ATM) during a cardiac cycle (viewing position: apex, view towards base), which was reconstructed from the displacement curves of the three apical scan planes (curves on the right). Black arrows indicate the assumed orientation of the three apical scan planes. Two open black circles indicate the measurement position to measure maximum amplitude and direction of apical motion. Colours code time intervals (yellow—IVC, red—ejection, green—IVR, blue—filling). Note the short septal motion of the apex early during IVC and the later lateral motion during ejection.

($\epsilon_{et}$) and during the entire cardiac cycle ($\epsilon_{tot}$) (*Figure 1*). Flow Doppler traces from the mitral and aortic valve were used to determine the time intervals of the cardiac cycle. Velocities are expressed in cm/s, motion in mm, strain rate in 1/s, and strain in %. The ECG served as common time base for all timing measurements with the beginning of QRS as reference. Timing data are expressed in ms or in per cent of the cardiac cycle.

## Calculation of apical transverse motion

A direct measurement of ATM is not possible with DMI, because the motion occurs perpendicular to the ultrasound beam. We therefore assumed the apex to behave as a 'cap' with homogeneous material properties where the different walls are pulling on. We used the longitudinal velocity traces of the apical segments to estimate the velocities of the 'cap rim' (*Figure 2A*). By integrating the velocity traces, motion was obtained. Curves from two opposite walls were averaged after inverting the anterior, lateral, or anteroseptal curve, respectively, in order to obtain transverse motion within each of the three apical scan planes (*Figure 2B*). Apical transverse motion perpendicular to the LV long axis was then reconstructed for the entire cardiac cycle assuming the scan planes of the three apical views to intersect at a 60° angle (*Figure 3*). Apical transverse motion was quantified by determining direction and amplitude of motion during the cardiac cycle and during systole. Data acquisition (J.U.V.) and analysis (T.M.S., M.S., E.G.) were done by different persons. Patient data were not available during analysis.

## Conventional parameters of ventricular asynchrony

Conventional parameters of inter- and intraventricular asynchrony were calculated according to the original publications. We obtained the delay in onset of aortic and pulmonary outflow [interventricular delay (IVD)[10,11]], the standard deviation of time-to-peak systolic velocity in the 12 mid- and basal segments (TsSD12[2]), the maximal dispersion in time-to-peak systolic velocity in basal segments of the two- or four-chamber view (SysDisp[3]), and in septal and lateral basal segments only (SLDisp[5]).

## Statistical analysis

Segmental timing, motion, and deformation data were grouped and averaged per patient prior to any statistical analyses to account for the clustered nature of these data. Data were presented as mean ± SD or median and inter-quartile range, as appropriate. Comparisons between groups were done by means of a *t*-test or Mann–Whitney U-test. For multiple groups, comparisons were made using analysis of variance or a Kruskal–Wallis test, with *post hoc* pairwise comparisons between the groups whereby adjustments to the significance level were made using the Tukey–Kramer method or Dunn's multiple comparison test, respectively. For the comparison of paired samples, a paired-test or Wilcoxon signed-rank test was used. Correlations between asynchrony parameters and regional function data were described by Pearson correlation coefficients. Receiver-operating-characteristics (ROC) curves and their area under the curve were calculated to assess the discriminative power of parameters.

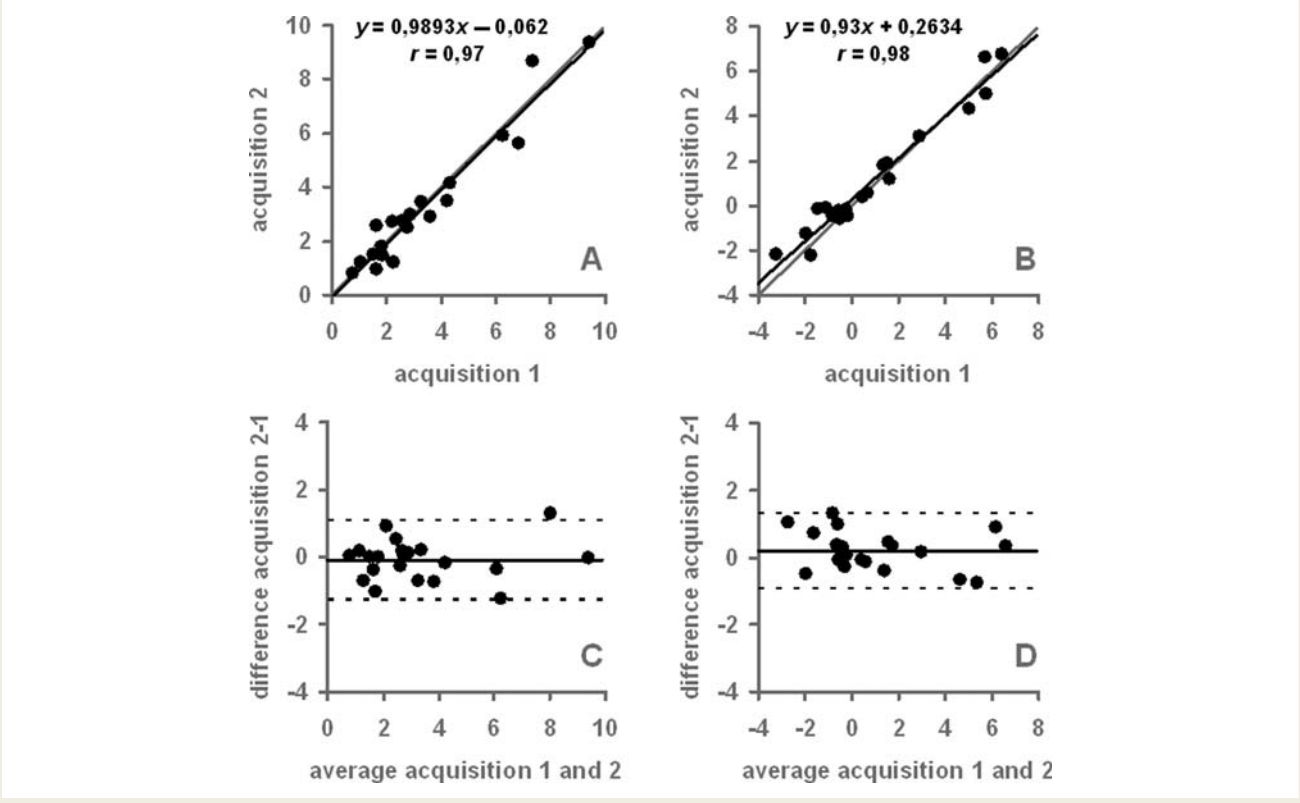


**Figure 4** Interobserver variability of $ATM_{4CV}$ estimates according to the proposed Doppler-based method in (mm). (*A*) $ATM_{4CV}$ during the entire cardiac cycle. (*B*) $ATM_{4CV}$ during ejection time. Solid black lines indicate the linear regression between readings, the grey lines the lines of identity. (*C* and *D*) Bland–Altmann plot of the same data. Solid black lines indicate the mean difference between readings (*C*: −0.10; *D*: +0.20), the dotted black lines the mean difference ± 1.96 • SD (*C*: −1.27 to 1.08; *D*: −0.93 to 1.33). The confidence interval of the latter was ± 0.05 in both plots.

AUC values were compared using the method offered by MedCalc. To determine the reproducibility of velocity, strain, and ATM estimations, 21 additional patients with different heart diseases were examined by two experienced observers at the beginning or the end of a regular echo examination. The agreement of measurements from both acquisitions was assessed according to the methods described by Bland and Altman. All statistical tests were two-sided and assessed at the 5% significance level. Owing to the exploratory nature of the study, no further adjustments were made to the significance level. We used the programs InStat 3 and Prism 4 (GraphPad Software Inc., La Jolla, USA) and MedCalc (MedCalc Software, Mariakerke, Belgium) for statistical calculations.

# Results

## Study population

Characteristics of the study population are given in *Table 1*. All patient groups had significantly wider QRS than NORM. Both LBBB groups had significantly reduced global LV function. Ischaemic LBBB patients had on average 3.5 infarcted segments. Thirty-eight per cent of the infarcted segments were localized in septal, anteroseptal, and anterior walls, 62% in lateral, posterior, and inferior regions. Thirty-six per cent of the infarcted segments were located in the apex, 33% in the mid, and 31% in the basal LV. Infarct scars were hypo- or akinetic, no dyskinesia was found. Average wall motion score was 1.35.

## Feasibility and reproducibility

From 1608 possible segmental and annular velocity traces, 1568 were recorded. Of those, 38 traces could not be analysed (97% feasibility). From 1176 possible segmental deformation traces, 111 could not be analysed (90% feasibility). Apical transverse motion could be calculated in 63 patients (94% feasibility).

Reproducibility of data acquisitions and readings of two experienced echocardiographers was tested. Segmental peak systolic velocity and time-to-peak velocity measurements correlated excellently ($r = 0.94$ and $r = 0.99$, respectively). Bland–Altman analysis revealed only minor differences (mean ± SD) 0.0 ± 0.6 cm/s and 1.4 ± 20.4 ms, respectively. Peak sys strain and time-to-peak strain correlated well ($r = 0.77$ and $r = 0.82$, respectively). Difference between readings (mean ± SD) was small (0.6 ± 3.3% and 0.0 ± 70 ms). $ATM_{4CV}$ estimates for the entire cardiac cycle ($r = 0.97$) as well as during ejection time ($r = 0.98$) correlated very well and differed only minimally between readings (mean ± SD) by 0.1 ± 0.6 and 0.2 ± 0.6 mm, respectively (*Figure 4*).

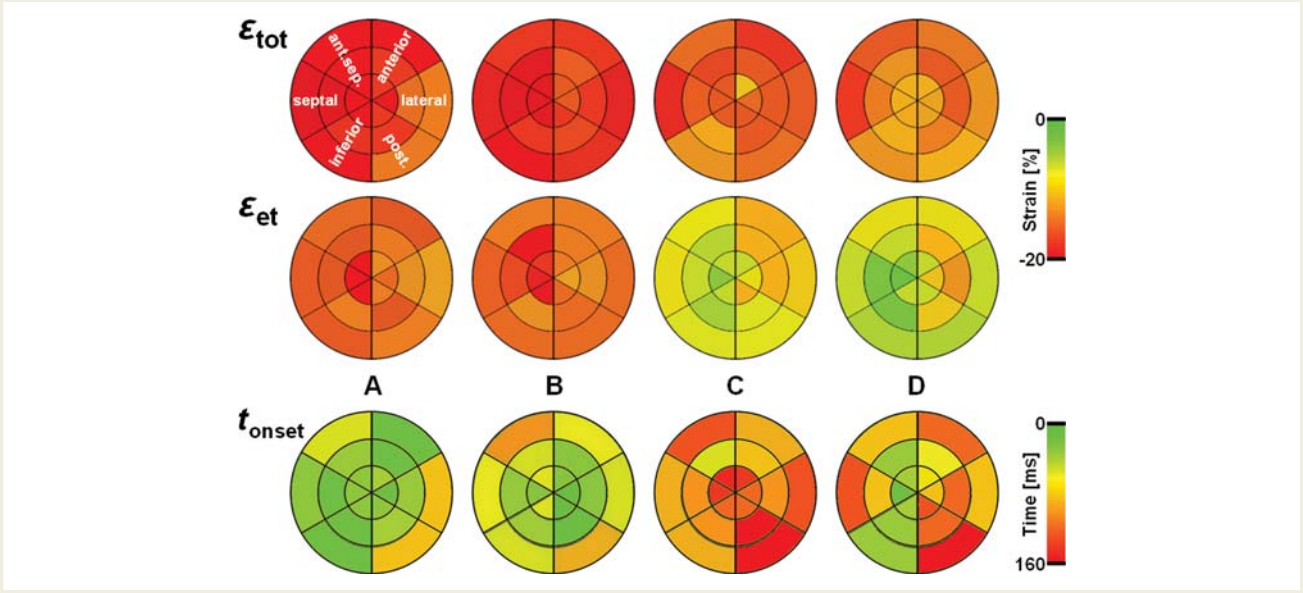


**Figure 5** Bull's eye displays of average regional strain distribution (first two rows) in (*A*) controls, (*B*) patients with RBBB, (*C*) non-ischaemic LBBB, and (*D*) ischaemic LBBB. Note the rather homogeneous distribution of the total myocardial deformation during the cardiac cycle ($\epsilon_{tot}$), while strain during ejection time ($\epsilon_{et}$) distribution differs between groups. In NORM and RBBB, $\epsilon_{et}$ is almost as high as $\epsilon_{tot}$ and more homogeneously distributed. In nLBBB, $\epsilon_{et}$ is lower and occurs predominantly in the left-sided regions of the LV. In iLBBB, the distribution is less homogeneous. The last row shows the temporal distribution of onset of shortening (see text for details).

**Table 2 Conventional parameters of asynchrony**

| | IVD | TsSD12 | SysDisp | SLDisp |
|---|---|---|---|---|
| NORM | 0 (−7 to 7) | 34 (12–49) | 49 (34–105) | 21 (9–60) |
| RBBB | 43 (30–48) | 33 (23–47) | 34 (13–61) | 17 (9–47) |
| nLBBB | −56 (−75 to −30)[a] | 55 (44–71)[a] | 92 (69–112) | 71 (50–95)[a] |
| iLBBB | −19 (−35 to −3) | 47 (31–57) | 49 (36–86) | 49 (27–86) |
| Cut-off[b] | 40 | 34.4 | 65 | 65 |

All values are given as median (and interquartile range in brackets) in (ms).
[a]significant difference vs. NORM. See text for further details.
[b]Cut-off to best distinguish responders and non-responders to CRT as suggested in the original publications.

## Temporal and regional distribution of myocardial function

In order to characterize the temporal and regional distribution of myocardial function, we measured the segmental onset of shortening ($t_{onset}$) as well as the amplitude of segmental shortening during ejection time ($\epsilon_{et}$) and during the total cardiac cycle ($\epsilon_{tot}$). In NORM, LV segmental shortening began shortly after QRS in the septal wall and spread over the LV within 25 ms. Right ventricular (RV) shortening occurred during the same time. Average shortening amplitude of LV segments was $\epsilon_{tot} = -19.0 \pm 2.1\%$ and $\epsilon_{et} = -14.8 \pm 2.3\%$. Inferior, septal, and anteroseptal walls showed on average significantly higher deformation values compared with the other walls ($\epsilon_{et(inf,sep,ans)} = -16.8 \pm 2.4\%$ vs. $\epsilon_{et(ant,lat,pos)} = -12.6 \pm 2.6\%$, $P < 0.001$) (*Figure 5A*).

In RBBB patients, onset of LV segmental shortening was earliest in the lateral wall, reaching the anteroseptum and the RV within 43 ms (no significant difference vs. NORM). The average shortening amplitude of LV segments was also similar ($\epsilon_{tot} = -18.2 \pm 2.4\%$, $\epsilon_{et} = -14.1 \pm 2.3\%$, both not significant vs. NORM). Distribution of strain between the walls was similar to NORM ($\epsilon_{et(inf,sep,ans)} = -15.6 \pm 2.8\%$ vs. $\epsilon_{et(ant,lat,pos)} = -12.7 \pm 2.4\%$, $P = 0.002$) (*Figure 5B*).

In nLBBB patients, shortening was earliest seen in the RV and spread over the heart reaching the LV posterior wall 144 ms later ($P < 0.001$ vs. NORM). The average LV segmental shortening was significantly reduced ($\epsilon_{tot} = -14.4 \pm 3.4\%$, $\epsilon_{et} = -7.4 \pm 3.4\%$, both $P < 0.001$ vs. NORM). The total strain amplitude did not differ between walls ($P = 0.655$), whereas the ejection time strain was inhomogeneous, with significantly lower average shortening of the inferior, septal, and anteroseptal walls compared with others ($\epsilon_{et(inf,sep,ans)} = -5.9 \pm 4.3\%$ vs. $\epsilon_{et(ant,lat,pos)} = -8.2 \pm 4.0\%$, $P = 0.002$) (*Figure 5C*).

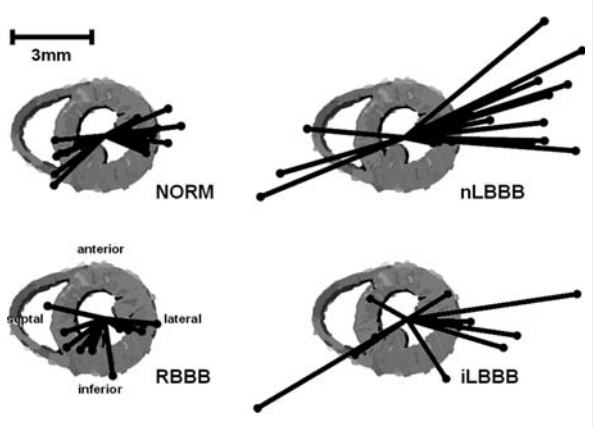


**Figure 6** Amplitude and direction of the main excursion of the ATM loop. The scale of 3 mm refers to the vectors, not to the icons of the ventricles. Note the predominant septal–lateral direction of ATM in nLBBB.

In iLBBB patients, onset of shortening showed a less clear distribution pattern and was less homogeneous. On average, shortening began in the septal or anteroseptal walls of the LV or in the RV and reached the posterior wall 105 ms later ($P < 0.001$ vs. NORM, $P < 0.01$ vs. nLBBB). Average LV segmental strain was reduced ($\epsilon_{tot} = -12.9 \pm 3.5\%$, $\epsilon_{et} = -7.3 \pm 3.0\%$, both $P < 0.001$ vs. NORM). Also in this group, total strain did not differ significantly between walls ($P = 0.509$). Differences in average ejection time strain between walls were significant ($\epsilon_{et(inf,sep,ans)} = -4.6 \pm 3.2\%$ vs. $\epsilon_{et(ant,lat,pos)} = -8.2 \pm 5.0\%$, $P = 0.015$) (*Figure 5D*).

## Conventional asynchrony parameters

SysDisp and SLDisp correlated weakly with EF in nLBBB ($r = 0.43$ and $r = 0.34$, respectively) and iLBBB groups ($r = 0.50$ and $r = 0.45$, respectively). SysDisp showed no significant difference among groups. TsSD12 and SLDisp revealed a significant difference only between NORM and nLBBB. IVD showed significant differences between all groups, except NORM vs. iLBBB. Results are summarized in *Table 2*.

## Apical transverse motion

Results are summarized in *Figures 6* and 7. In NORM, the motion of the apex was very low [median 1.8 (1.5–2.0) mm]. Apical transverse motion was also very low in patients with RBBB [median 1.5 (1.3–1.9) mm] and not significantly different compared with NORM ($P = 0.999$). Patients with nLBBB showed a pronounced motion of the apex, significantly different vs. NORM and RBBB [median 4.3 (2.7–5.6) mm, both $P < 0.001$]. Typically, a short-lived motion towards the septum was seen during IVCT (*Figure 3*, yellow part of the curve). During ejection time, the apex moved laterally (*Figure 3*, red part of the curve). In the group of iLBBB, only two patients showed a behaviour similar to nLBBB, otherwise the ATM in this group was as low as in NORM and RBBB [2.4 (1.9–4.0) mm, $P = 0.183$ vs. NORM, $P = 0.037$ vs. RBBB] (*Figure 7A*).

Direction of ATM main excursion was, in general, close to the septal–lateral plane, i.e. the 4CV scan plane. We therefore tested ATM in this plane only ($ATM_{4CV}$). $ATM_{4CV}$ values differed only slightly from ATM. Also in $ATM_{4CV}$, nLBBB patients showed significantly more apical motion than NORM and RBBB [NORM 1.6 (1.0–2.0) mm; RBBB 1.1 (0.8–1.5) mm, $P = 0.999$ vs. NORM; nLBBB 4.0 (2.6–4.9) mm, $P < 0.001$ vs. NORM and RBBB], whereas iLBBB showed significantly more apical motion compared with RBBB patients [2.1 (1.8–3.4) mm, $P = 0.114$ vs. NORM, $P = 0.022$ vs. RBBB] (*Figure 7B*). On average, $ATM_{4CV}$ during ejection time ($ATM_{4CV\text{-}et}$) showed comparable relations, but lower motion amplitudes.

$ATM_{4CV}$ did not correlate with QRS width (all $r < 0.15$) or EF (all $r < 0.25$) within the groups of NORM, RBBB, and LBBB.

To further analyse the relation of ATM towards regional contraction inhomogeneity within the LV, we calculated the difference between the averaged strains of the septal and lateral wall segments during ejection time ($\varepsilon_{diff} = \overline{\varepsilon_{et\,(lat)}} - \overline{\varepsilon_{et\,(sep)}}$). We found a significant correlation of $ATM_{4CV}$ with this marker of regional function inhomogeneity ($r = 0.74$, CI 0.57–0.85, $P < 0.001$). Only IVD correlated (weaker) as well, whereas none of the conventional asynchrony parameters showed a relevant correlation to this marker of regional function inhomogeneity (*Figure 8*).

The ROC analysis for the distinction between NORM and LBBB groups revealed for $ATM_{4CV}$ an area under the curve of 0.87 (CI 0.78–0.97, $P < 0.001$). See *Figure 9* for comparison to conventional tissue velocity-based parameters.

# Discussion

## Main findings of the study

In this study, we could demonstrate inhomogeneities in temporal and regional distribution of myocardial shortening, particularly during ejection time, which differed among healthy volunteers and patients with different conduction delays.

We introduced the new parameter of ATM. We could show that ATM estimation by means of tissue Doppler echocardiography is technically feasible and reproducible and that it allows to quantify and distinguish typical motion patterns of the LV. Apical transverse motion was strongly related to LV temporal and regional function inhomogeneities and summarized them in a single parameter. Apical transverse motion could distinguish well between NORM and LBBB study groups.

## Temporal and regional function inhomogeneities

Our findings confirm earlier works in animals[1,12] and humans,[13,14] which reported a delayed onset of systolic shortening in the lateral and posterior LV region of patients with LBBB. They also confirm that in LBBB, the lateral and posterior walls contract mainly during ejection,[12] whereas septal regions of the LV shorten very early and, thus, can hardly contribute to the stroke work. We found that the average ejection time strain per wall mirrors these conditions well: in NORM and RBBB, the $\epsilon_{et}$-differences between walls were low with slightly higher values in the septal region, whereas LBBB patients revealed a significant imbalance in $\epsilon_{et}$ favouring the lateral wall. We found a significantly time delay in onset of regional shortening in the lateral region of nLBBB patients. This relation was less pronounced in LBBB patients with ischaemic background,

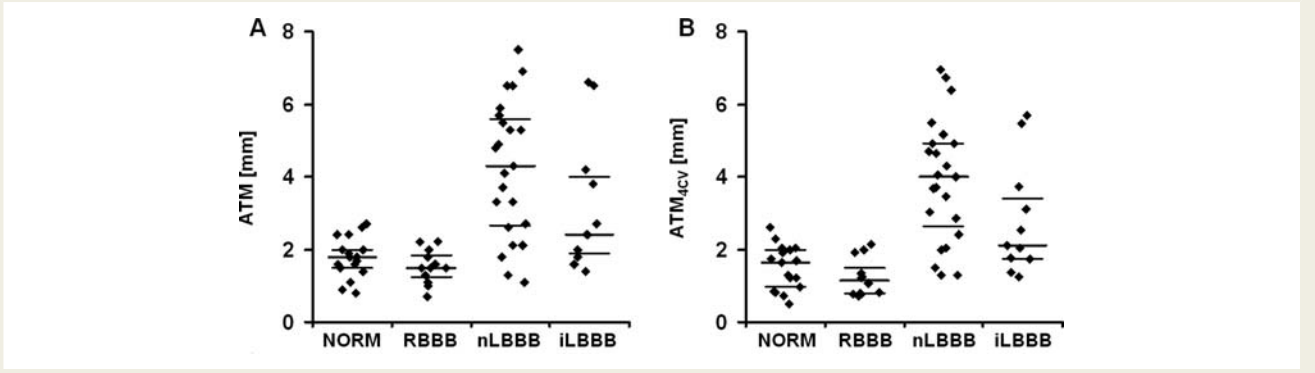


**Figure 7** Amplitude of ATM measured as (*A*) maximum excursion in any direction during the cardiac cycle and (*B*) motion amplitude within the 4CV plane only ($ATM_{4CV}$). Bold black indicates the median, thin lines the first and third quartile.

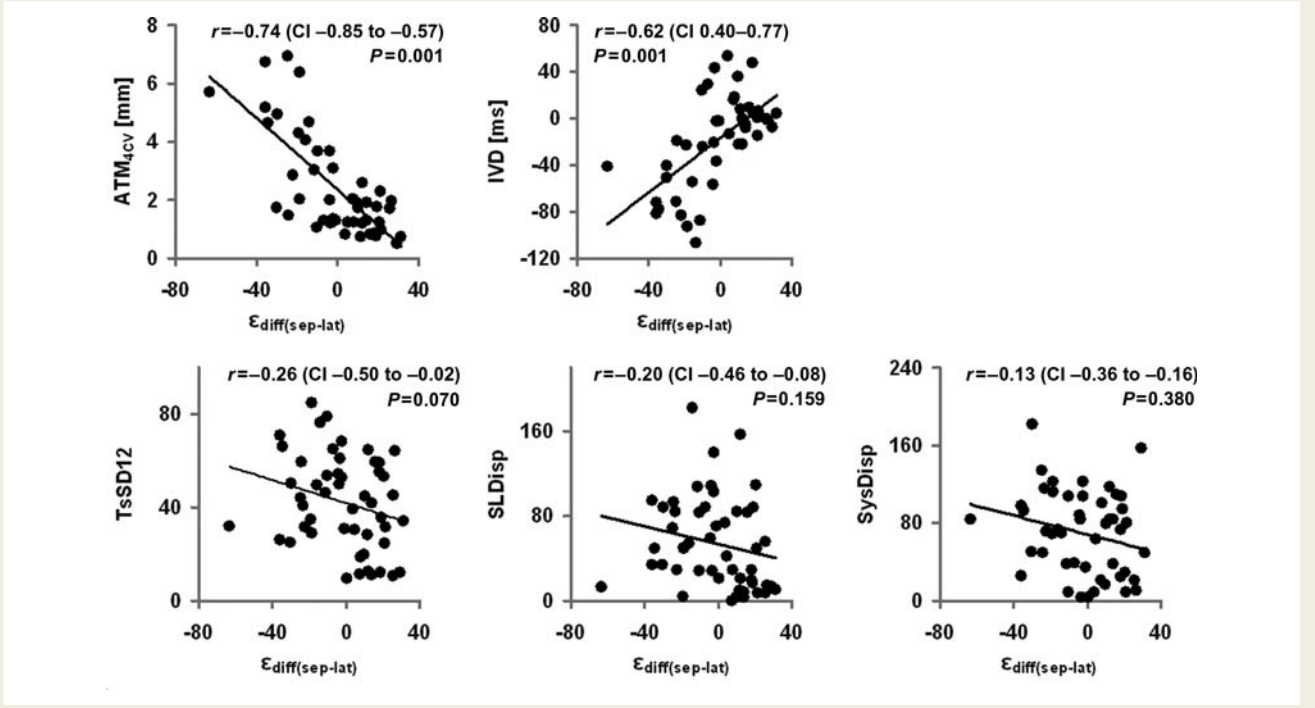


**Figure 8** Correlation between the difference of the summed septal and lateral segmental ejection time strains as parameter of LV functional and temporal inhomogeneity and $ATM_{4CV}$, IVD as well as different conventional tissue-Doppler-based dyssynchrony parameters.

which may be attributed to the different location and extent of infarct scar in this group.

## Conventional asynchrony parameters

To estimate this temporal and functional LV inhomogeneities in our patients, we choose Doppler- and tissue-Doppler-based parameters which were previously suggested for use in the context of CRT.[2,3,5,10,11] Although our study population was not investigated with the intention to predict CRT response, it may be assumed that those parameters are able to reflect LV asynchrony.

IVD showed differences between groups and correlated weakly with the septal–lateral strain difference. TsSD12 was significantly prolonged in nLBBB. No other significant difference was detected by the tissue-Doppler-based parameters (*Table 2*). None of the tissue-Doppler-based parameters correlated significantly with the septal–lateral strain difference (*Figure 8*). We conclude, thus, that the conventional tissue-Doppler-based asynchrony parameters may in part reflect temporal asynchrony, but do not directly reflect inhomogeneities of regional LV function.

## Apical transverse motion

In this study, we suggest for the first time to use the new parameter of ATM for the assessment of LV asynchrony. We hypothesize that apical motion is a surrogate parameter,

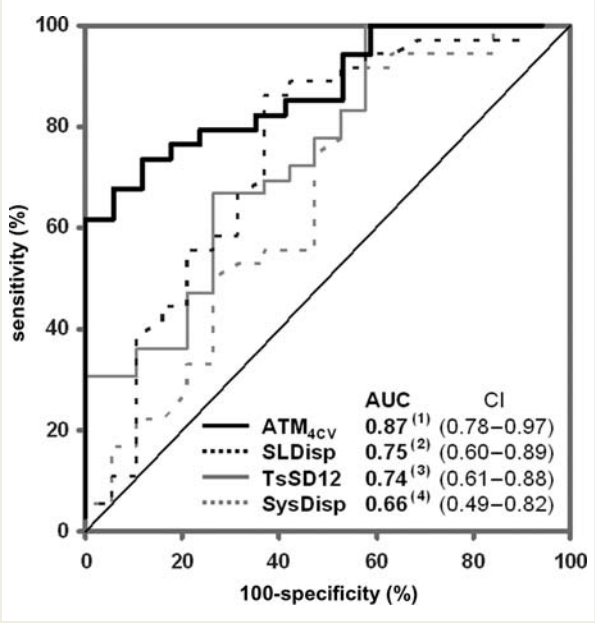


**Figure 9** Receiver-operating-characteristic analysis for $ATM_{4CV}$.and different conventional Doppler based dyssynchrony parameters for the distinction between NORM and LBBB patient groups. Significance levels are (1) $P < 0.001$, (2) $P = 0.003$ ($P = 0.1532$ vs. $ATM_{4CV}$), (3) $P = 0.003$ ($P = 0.1322$ vs. $ATM_{4CV}$), (4)$P = 0.058$ ($P = 0.0221$ vs. $ATM_{4CV}$).

comprising information on both regional myocardial function inhomogeneities and temporal inhomogeneities of myocardial contraction due to activation delays. Thus, a pronounced apical motion ('apical rocking') will occur, if either one of two opposing wall contracts weaker (e.g. scar tissue) or delayed (conduction delay).

This is supported by the facts that ATM correlates well with the septal–lateral difference in myocardial wall strain as a marker of function inhomogeneities and that ATM showed different typical apical motion patterns in different conduction delays. It, furthermore, could distinguish between the normal hearts and LBBB patients with and without scars.

Given the good reproducibility of the ATM measurements, the scatter of ATM within the LBBB groups may be interpreted as a confirmation that mechanical and electrical dyssynchrony are only loosely related.[15]

## Potential advantages of apical transverse motion

Apical transverse motion appears to better reflect the true sequence of regional myocardial shortening in the LV walls and the different magnitudes of deformation. It may, therefore, be used to characterize different entities of LV pathology better than with traditional, velocity peak timing-based methods. This may be of an advantage in analysing LV dyssynchrony and in selecting CRT candidates.

## Limitations

The assessment of ATM was tissue-Doppler-based, assuming that the apex behaves as a homogeneous 'cap'. A more direct assessment using modern speckle tracking approaches was not feasible due to the inherent image artefacts in the apex region. Furthermore, the chosen way of ATM estimation is theoretically more resistant to an overall sideward motion of the LV than tracking based approaches, since tissue-Doppler data are collected more longitudinally and are, thus, not influenced by a possible sideward component of myocardial motion.

Apical transverse motion could not be validated against a gold standard. Such a direct validation proved to be difficult because of the lack of a gold standard method. In particular, MRI tagging was attempted, but failed due to the flawed signals in the thin apical myocardium, the insufficient temporal and spatial resolution of the method, and the influence of the above mentioned overall heart motion. Echocardiographic tracking methods are frequently disturbed by the stationary artefacts in the apical region. Ultrasonic crystals would be an option, but cannot be used in humans, would influence the apical motion due to the open pericardium procedure, and would theoretically also be subject to overall heart motion interference.

Since ATM was shown to be related to functional inhomogeneities in LV walls, a relation between ATM and the extend and location of myocardial scar tissue must be expected. Our study is underpowered to address this specific question which leaves room for further investigation.

The mean age of our control group was lower than the age of the patients. We therefore performed a sub-analysis of our data which compared $ATM_{4CV}$ of volunteers $<30$ years and $>50$ years, which revealed no significant differences ($1.47 \pm 0.65$ mm vs. $1.61 \pm 0.38$ mm, $P = 0.640$). Furthermore, we noted no correlation between age of the volunteers and $ATM_{4CV}$ ($r = 0.12$).

## Conclusion

Apical transverse motion is a new and simple parameter of LV asynchrony. It integrates information on both regional and temporal function inhomogeneities of the LV and, thus, may be used to assess LV asynchrony in the clinical context. Our data suggest that ATM has the ability to differentiate patients with differing function and conduction abnormalities. Apical transverse motion estimation is feasible and well reproducible. Further studies will determine its potential role in predicting response to CRT.

## Funding

This work was in part supported by a research grant of the University Erlangen (ELAN 04.09.09.1).

**Conflict of interest:** none declared.

## References

1. van Oosterhout MF, Arts T, Muijtjens AM, Reneman RS, Prinzen FW. Remodeling by ventricular pacing in hypertrophying dog hearts. *Cardiovasc Res* 2001;**49**: 771–778.
2. Yu CM, Zhang Q, Fung JW, Chan HC, Chan YS, Yip GW, Kong SL, Lin H, Zhang Y, Sanderson JE. A novel tool to assess systolic asynchrony and identify responders of cardiac resynchronization therapy by tissue synchronization imaging. *J Am Coll Cardiol* 2005;**45**:677–684.

3. Bax JJ, Bleeker GB, Marwick TH, Molhoek SG, Boersma E, Steendijk P, van der Wall EE, Schalij MJ. Left ventricular dyssynchrony predicts response and prognosis after cardiac resynchronization therapy. *J Am Coll Cardiol* 2004;**44**:1834–1840.
4. Gorcsan J III, Kanzaki H, Bazaz R, Dohi K, Schwartzman D. Usefulness of echocardiographic tissue synchronization imaging to predict acute response to cardiac resynchronization therapy. *Am J Cardiol* 2004;**93**:1178–1181.
5. Van de Veire NR, Bleeker GB, De Sutter J, Ypenburg C, Holman ER, van der Wal EE, Schalij MJ, Bax JJ. Tissue synchronisation imaging accurately measures left ventricular dyssynchrony and predicts response to cardiac resynchronisation therapy. *Heart* 2007;**93**:1034–1039.
6. Notabartolo D, Merlino JD, Smith AL, DeLurgio DB, Vera FV, Easley KA, Martin RP, León AR. Usefulness of the peak velocity difference by tissue Doppler imaging technique as an effective predictor of response to cardiac resynchronization therapy. *Am J Cardiol* 2004;**94**:817–820.
7. Chung ES, Leon AR, Tavazzi L, Sun JP, Nihoyannopoulos P, Merlino J, Abraham WT, Ghio S, Leclercq C, Bax JJ, Yu CM, Gorcsan J III, St John Sutton M, De Sutter J, Murillo J. Results of the Predictors of Response to CRT (PROSPECT) trial. *Circulation* 2008;**117**:2608–2616.
8. Kapetanakis S, Kearney MT, Siva A, Gall N, Cooklin M, Monaghan MJ. Real-time three-dimensional echocardiography: a novel technique to quantify global left ventricular mechanical dyssynchrony. *Circulation* 2005;**112**:992–1000.
9. Mele D, Pasanisi G, Capasso F, De Simone A, Morales MA, Poggio D, Capucci A, Tabacchi G, Sallusti L, Ferrari R. Left intraventricular myocardial deformation dyssynchrony identifies responders to cardiac resynchronization therapy in patients with heart failure. *Eur Heart J* 2006;**27**:1070–1078.
10. Cleland JG, Daubert JC, Erdmann E, Freemantle N, Gras D, Kappenberger L, Klein W, Tavazzi L, CARE-HF study Steering Committee Investigators. The CARE-HF study (CArdiac REsynchronisation in Heart Failure study): rationale, design and end-points. *Eur J Heart Fail* 2001;**3**:481–489.
11. St John Sutton MG, Plappert T, Abraham WT, Smith AL, DeLurgio DB, Leon AR, Loh E, Kocovic DZ, Fisher WG, Ellestad M, Messenger J, Kruger K, Hilpisch KE, Hill MR, Multicenter InSync Randomized Clinical Evaluation (MIRACLE) study group. Effect of cardiac resynchronization therapy on left ventricular size and function in chronic heart failure. *Circulation* 2003;**107**:1985–1990.
12. Vernooy K, Verbeek XA, Peschar M, Prinzen FW. Relation between abnormal ventricular impulse conduction and heart failure. *J Interv Cardiol* 2003;**16**:557–562.
13. Zwanenburg JJ, Götte MJ, Marcus JT, Kuijer JP, Knaapen P, Heethaar RM, van Rossum AC. Propagation of onset and peak time of myocardial shortening in time of myocardial shortening in ischaemic versus nonischemic cardiomyopathy: assessment by magnetic resonance imaging myocardial tagging. *J Am Coll Cardiol* 2005;**46**:2215–2222.
14. Nelson GS, Berger RD, Fetics BJ, Talbot M, Spinelli JC, Hare JM, Kass DA. Left ventricular or biventricular pacing improves cardiac function at diminished energy cost in patients with dilated cardiomyopathy and left bundle-branch block. *Circulation* 2000;**102**:3053–3059.
15. Bleeker GB, Schalij MJ, Molhoek SG, Verwey HF, Holman ER, Boersma E, Steendijk P, Van Der Wall EE, Bax JJ. Relationship between QRS duration and left ventricular dyssynchrony in patients with end-stage heart failure. *J Cardiovasc Electrophysiol* 2004;**15**:544–549.